Do the TRAPPIST-1 Planets Have Hydrogen-rich Atmospheres?

Yasunori Hori[1,2] and Masahiro Ogihara[2]
[1] Astrobiology Center, 2-21-1 Osawa, Mitaka, Tokyo 1818588, Japan; yasunori.hori@nao.ac.jp
[2] National Astronomical Observatory of Japan, 2-21-1 Osawa, Mitaka, Tokyo 1818588, Japan

Abstract

Recently, transmission spectroscopy in the atmospheres of the TRAPPIST-1 planets revealed flat and featureless absorption spectra, which rule out cloud-free, hydrogen-dominated atmospheres. Earth-sized planets orbiting TRAPPIST-1 likely have either a clear or a cloudy/hazy, hydrogen-poor atmosphere. In this paper, we investigate whether a proposed formation scenario is consistent with expected atmospheric compositions of the TRAPPIST-1 planets. We examine the amount of hydrogen-rich gas that TRAPPIST-1-like planets accreted from the ambient disk until disk dispersal. Since TRAPPIST-1 planets are trapped into a resonant chain, we simulate disk gas accretion onto a migrating TRAPPIST-1-like planet. We find that the amount of accreted hydrogen-rich gas is as small as 10^{-2} wt% and 0.1 wt% for TRAPPIST-1 b and 1 c, 10^{-2} wt% for 1 d, 1 wt% for 1 e, a few wt% for 1 f and 1 g and 1 wt% for 1 h, respectively. We also calculate the long-term thermal evolution of TRAPPIST-1-like planets after disk dissipation and estimate the mass loss of their hydrogen-rich atmospheres driven by stellar X-ray and UV irradiation. We find that all the accreted hydrogen-rich atmospheres can be lost via hydrodynamic escape. Therefore, we conclude that TRAPPIST-1 planets should have no primordial hydrogen-rich gases but secondary atmospheres such as a Venus-like one and water vapor, if they currently retain atmospheres.

Unified Astronomy Thesaurus concepts: Exoplanet formation (492); Exoplanet atmospheres (487); Exoplanets (498); Planet formation (1241)

1. Introduction

TRAPPIST-1 is an ultracool red dwarf with mass of $0.089\,M_\odot$ near the boundary between brown dwarfs and stars (Delrez et al. 2018; Van Grootel et al. 2018), located 12.43 pc[3] away from Earth. Recently, seven Earth-sized planets orbiting TRAPPIST-1 were reported (Gillon et al. 2016, 2017), three of which dwell in the conventional habitable zone. Transit timing variation analyses of the TRAPPIST-1 planets find that their masses range from Mars to Earth (Gillon et al. 2017; Wang et al. 2017; Grimm et al. 2018). The TRAPPIST-1 planets are suited for studying atmospheric characterization and habitability of terrestrial planets beyond the solar system.

The low densities of the TRAPPIST-1 planets (see Table 1) may conceal substantial volatile content, e.g., water inside their cores. Monte Carlo studies on their internal compositions suggest that the inner planets have a small water content (Quarles et al. 2017; Grimm et al. 2018), which depends on their core-to-mantle mass ratio (Dorn et al. 2018; Suissa & Kipping 2018; Unterborn et al. 2018a, 2018b). Interior modeling of the TRAPPIST-1 planets using updated masses indicates that the mass fractions of water might be uniform or increase with semimajor axis ($\lesssim 25$ wt%) (Dorn et al. 2018). The current locations of the six inner TRAPPIST-1 planets are inside a snow line. Their volatile reservoirs should come from inward transport of building blocks such as icy pebbles (Ida et al. 2019) or cometary material (Kral et al. 2018) and planetary embryos that formed outside. In fact, the six inner planets are trapped into a resonant chain; the outermost planet, TRAPPIST-1 h, may form the Laplace relations (Luger et al. 2017). In addition, transit geometry of the TRAPPIST-1 planets shows that they are in a nearly edge-on, co-planar system. The orbital architecture of the co-planar, resonant TRAPPIST-1

system supports that the planets experienced orbital migration (e.g., Mills et al. 2016; Ormel et al. 2017; Papaloizou et al. 2018). A disk migration scenario is favorable to explain the long-lived dynamical stability of the tightly packed TRAPPIST-1 system (Matsumoto et al. 2012; Tamayo et al. 2017), which depends on the strength of tidal interactions between the inner planets and the central star (Papaloizou et al. 2018).

Hubble Space Telescope (*HST*)/Wide Field Camera 3 (WFC3) measurements exhibit no prominent absorption features at near-infrared wavelengths in transmission spectra of six of the TRAPPIST-1 planets (de Wit et al. 2016, 2018; Zhang et al. 2018; Burdanov et al. 2019).[4] The combined spectrum of the planets rules out cloud-free, hydrogen-dominated atmospheres, except for TRAPPIST-1 f and 1 g (de Wit et al. 2018; Moran et al. 2018); Wakeford et al. (2019) recently suggested that a clear hydrogen-dominated atmosphere may be ruled out for TRAPPIST-1 g. Since high-altitude clouds and haze are not expected to form in hydrogen-dominated atmospheres around temperate planets (e.g., Morley et al. 2015), transit spectroscopy of the TRAPPIST-1 planets suggests no atmosphere or a high-metallicity atmosphere referred to as a secondary atmosphere. Future observations with precision higher than 20 ppm is, however, needed to distinguish between the effects of cloud/haze and high metallicity in the atmospheres (Moran et al. 2018). Secondary atmospheres of the inner TRAPPIST-1 planets (1 b and 1 c) may be replenished with volcanic activity and outgassing from magma ocean due to electromagnetic induction heating (Kislyakova et al. 2017) and tidal heating (Barr et al. 2018).

Atmospheric spectroscopy of the TRAPPIST-1 planets suggests that at least five of them may not retain primordial

---

[3] The parallax of TRAPPIST-1 from the *Gaia* mission: *Gaia* DR2 archive (https://gea.esac.esa.int/archive/).

[4] Stellar contamination effects on transmission spectra are expected to be less significant than those predicted in Zhang et al. (2018) (Ducrot et al. 2018; Morris et al. 2018a, 2018b).

Table 1
Observed Physical Properties of the TRAPPIST-1 Planets (Grimm et al. 2018)

Planet	Mass ($M_\oplus$)	Radius ($R_\oplus$)	Density ($\rho_\oplus$)	Semimajor Axis (au)
b	1.017	1.121	0.726	0.01154775
c	1.156	1.095	0.883	0.01581512
d	0.297	0.784	0.616	0.02228038
e	0.772	0.910	1.024	0.02928285
f	0.934	1.046	0.816	0.03853361
g	1.148	1.148	0.759	0.04687692
h	0.331	0.773	0.719	0.06193488

atmospheres at present. In this paper, we investigate whether a proposed formation scenario is consistent with expected atmospheric compositions of the TRAPPIST-1 planets. There are two processes that we consider in this study: accretion of hydrogen-dominated disk gas onto a planetary core during orbital migration and atmospheric loss from a planet by photoevaporation. In Section 2, we present a disk model and numerical prescriptions of gas accretion onto a migrating planetary core. In Section 3, we show the amount of hydrogen-rich atmosphere that TRAPPIST-1 like planets can acquire in situ and during orbital migration, and then estimate photoevaporative loss of the accreted hydrogen-rich gases from TRAPPIST-1-like planets. In Section 4, we compare our results with atmospheric properties of the TRAPPIST-1 planets predicted by transmission spectroscopy and discuss the atmospheric compositions of the TRAPPIST-1 planets and their origins. We summarize our results in the last section.

2. Methods

2.1. A Migrating Planet

We consider an isolated planetary core with mass 0.3, 0.7, and 1 $M_\oplus$ to be embedded in a disk. A planetary core initially resides inside/outside a snow line ($\sim$0.062 au) around TRAPPIST-1 ($L_\star/L_\odot = 5.24 \times 10^{-4}$, where $L_\star$ is the stellar luminosity) and then accretes a disk gas in situ or during orbital migration. Since planetary accretion proceeds rapidly in an inner region, their building blocks should be almost depleted there before a planetary core starts migrating inward, although neighboring embryos may collide with each other during resonance trapping and/or orbital migration. In fact, a planetary embryo can quickly grow up to the pebble isolation mass (Lambrechts et al. 2014; Schoonenberg et al. 2019) in a high pebble-mass flux (Lambrechts et al. 2019). We assume that planetesimal/pebble accretion onto a planetary core ceases during orbital excursion, which allows us to estimate the maximum amount of accreting hydrogen-rich gas.

We adopt torque formulae of Type I migration, including thermal torques, on a low-mass planet in a three-dimensional and non-isothermal disk (Benítez-Llambay et al. 2015; Jiménez & Masset 2017; Masset 2017; Guilera et al. 2019). The thermal torque is the sum of the cold and heating torque. Since we assume no accretion of pebbles/planetesimals onto a planet, the heating torque comes from gas accretion processes. As shown in Section 3, the total amount of accreted disk gas onto TRAPPIST-1-like Earth-sized planets is less than a few wt% of their total masses. The heating torque newly included in this study does not make a significant contribution to planetary migration. A timescale of orbital migration is almost comparable to that of radiative diffusion, i.e., gravitational contraction

of a planet, in our simulations. As seen in Figure 1, the envelope evolution of a migrating planet mostly occurs after it gets stalled at a resonant location. Thus, we assume that a migrating planet can be thermodynamically equilibrated with the ambient disk gas. In addition, the TRAPPIST-1 planets are unlikely to undergo a giant impact phase after disk dispersal as seen in the inner solar system because of resonant capture (Ormel et al. 2017). Thus, atmospheric mass loss via giant impacts in the late stage of planet assembly can be neglected.

2.2. Disk Model

An initial disk model adopts the surface density profile given in Andrews et al. (2010):

$$\Sigma_{\rm gas} = \Sigma_0 \left(\frac{r}{R_{\rm c}}\right)^{-1} \exp\left(-\frac{r}{R_{\rm c}}\right), \qquad (1)$$

where $\Sigma_{\rm gas}$ is the surface density of a disk gas, r is the distance from a central star, $R_{\rm c}$ is the characteristic disk radius, and Σ_0 is the initial surface density of a disk at $r = R_{\rm c}$, which is determined by the initial mass and size of a disk. We adopt a radial profile of a midplane temperature in a disk with a constant h used in Ormel et al. (2017):

$$T(r) = 180 \left(\frac{M_\star}{0.08\,M_\odot}\right)\left(\frac{h}{0.03}\right)^2\left(\frac{r}{0.1\,{\rm au}}\right)^{-1}, \qquad (2)$$

where $M_\star$ is the mass of a central star and h is the inner disk aspect ratio. Disk accretion rates for M-type stars were estimated to be 10^{-9}–$10^{-10} M_\odot$ yr^{-1} (e.g., Manara et al. 2015). A midplane temperature in a disk with such a low accretion rate is little changed with time (see, e.g., Bitsch et al. 2015). Thus, we consider a fixed disk temperature profile in this study.

We consider that a disk is initially truncated at 100 au and the initial disk mass ($M_{\rm disk}$) is proportional to the stellar mass (Andrews et al. 2013); $M_{\rm disk} = 0.1\,M_\star$, which is gravitationally stable (see Equation (3) in Kratter & Lodato 2016). Given that the dust-to-gas ratio is 0.011 according to [Fe/H] = +0.04 of TRAPPIST-1 (Gillon et al. 2016), an initial amount of solid material of $\sim$32.6 $M_\oplus$ is available for planet formation around TRAPPIST-1 star.[5] Using an empirical $M_{\rm disk}$–$R_{\rm c}$ relation[6] (Andrews et al. 2010), we find that $R_{\rm c} \sim 25.4$ au.

We assume that the inner edge of a disk, $r_{\rm in}$, is given by the magnetospheric cavity radius (Frank et al. 1992); Ormel et al. (2017) estimated $r_{\rm in} \sim 0.01$ au which is close to the current location of the innermost planet. The surface density of a disk gas declines exponentially with time, i.e., $\Sigma_{\rm gas}(t) = \Sigma_{\rm gas}(t = 0)\exp(-t/\tau_{\rm disk})$, where t is the time and $\tau_{\rm disk}$ corresponds to the timescale of disk dispersal. We adopt $\tau_{\rm disk} = 2.5$ Myr based on disk lifetimes estimated from age–disk fraction relations in young star clusters (Haisch et al. 2001; Hernández et al. 2008; Mamajek 2009; Fedele et al. 2010; Ribas et al. 2014). We consider two disk evolution models in this study: (i) a steady-state, viscous accretion disk and (ii) a disk wind-driven accretion disk (Suzuki & Inutsuka 2009). In the former case, we do not simulate time evolution of the

---

[5] Since N-body-simulations of TRAPPIST-1 planets predict a high efficiency of planet formation (Schoonenberg et al. 2019), our disk model can reconcile the total mass of the TRAPPIST-1 planets.

[6] $\frac{M_{\rm disk}}{M_\odot} \sim 2 \times 10^{-3}\left(\frac{R_{\rm c}}{10\,{\rm au}}\right)^{1.6}$.
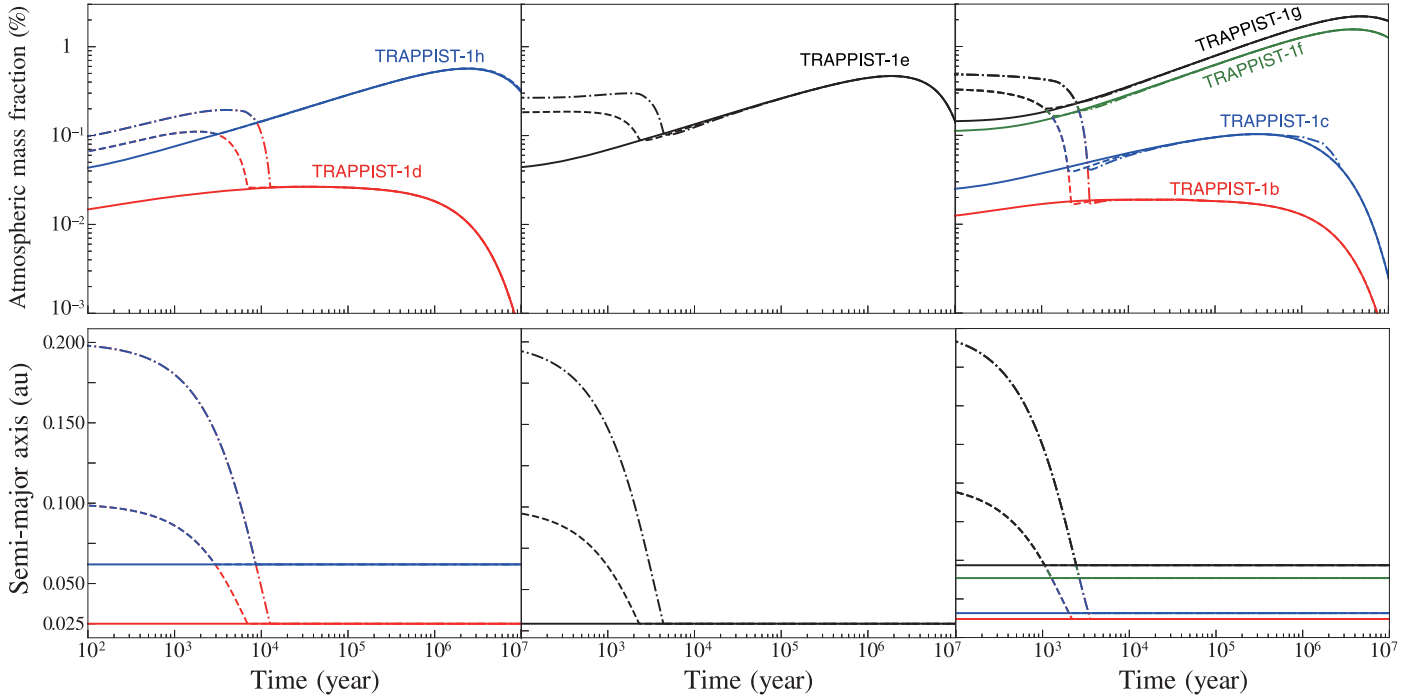
Figure 1. Time evolution of the atmospheric mass fraction (top) and semimajor axis (bottom) of a non-migrating (solid curves) and migrating planetary core with mass of 0.3 $M_{\oplus}$ (left: TRAPPIST-1 d (red), 1 h (blue)), 0.7 $M_{\oplus}$ (middle: 1 e), and 1 $M_{\oplus}$ (right: 1 b (red), 1 c (blue), 1 f (green), and 1 g (black)). A planetary core starts to migrate from 0.1 au (dashed ones) or 0.2 au (dashed–dotted ones). The locations of a non-migrating planetary core adopt semimajor axes similar to those of the TRAPPIST-1 planets. Mass loss from an accreting planet driven by a stellar XUV irradiation is not included.

surface density of a disk gas. Instead, we simply use an exponential decay of $\Sigma_{\mathrm{gas}}(t)$. Regarding the rapidly dissipating disk, it is pointed out that effects of disk winds (Suzuki & Inutsuka 2009; Suzuki et al. 2016; Ogihara et al. 2018) or photoevaporation (Alexander et al. 2014) or both mechanisms trigger a rapid disk dispersal. For the latter case, we introduce a two-stage disk dispersal, namely, $\tau(t > \tau_{\mathrm{disk}}) = 10$ kyr.

2.3. Gas Accretion onto a Planet

A disk gas mainly consists of hydrogen and helium. We calculate time-dependent accretion rates of the disk gas onto a planetary core using one-dimensional hydrodynamic simulations and then estimate the mass of the hydrogen-rich atmosphere that it acquires before the disk gas disappears. We briefly present numerical prescriptions of our hydrodynamic simulations (see also Ikoma & Hori 2012). A quasi-hydrostatic evolution of a planet is described by

$$\frac{\partial P}{\partial M} = -\frac{GM}{4\pi r^4}, \tag{3}$$

$$\frac{\partial r}{\partial M} = \frac{1}{4\pi r^2 \rho}, \tag{4}$$

$$\frac{\partial T}{\partial M} = \frac{T}{P}\nabla\frac{\partial P}{\partial M}, \tag{5}$$

$$\frac{\partial L}{\partial M} = -T\frac{dS}{dt}, \tag{6}$$

where M, P, T, ρ, L, and S are the mass enclosed within a radius, r, pressure, temperature, density, luminosity, and specific entropy, respectively. ∇ is the temperature gradient, which is determined by heat transfer. The luminosity at the core surface, L_{radio}, is the luminosity due to the radioactive decay of

chondrites as core material, $L_{\mathrm{radio}} = 2 \times 10^{20}(M_{\mathrm{core}}/M_{\oplus})$ erg s^{-1}, where M_{core} is the rocky core mass of a planet (see Guillot et al. 1995). Core cooling delays the gravitational contraction of a planet, leading to less H_2/He envelope mass. We integrate Equations (3)–(6) to determine the interior structure of a planet at a given time. The outer boundary conditions for an accreting planet are defined by temperature and density at the Hill radius, which are thermodynamically equilibrated with those of a disk gas. Gravitational potential energy released by the contraction/expansion of a planetary atmosphere should compensate for heat energy which is carried away into space by radiation. Thus, we calculate the mass change of a planet that undergoes thermal evolution.

In this study, planets are not massive enough to open a gap in the ambient disk, namely, $R_{\mathrm{H}} < H_{\mathrm{p}}$ and $M_{\mathrm{p}} < 40\nu M_{\star}/(r^2\Omega)$ (Lin & Papaloizou 1993), where we assume an α-disk model with a disk viscosity parameter $\alpha = 10^{-3}$ (Shakura & Sunyaev 1973), R_{H} is the Hill radius of a planet, H_{p} is the pressure scale height of a disk gas, M_{p} is the planetary mass, $M_{\star}$ is the stellar mass, Ω is the Keplerian angular velocity, ν is the kinematic viscosity given by $\nu = \alpha h^2 r^2 \Omega$, and h is the disk aspect ratio. Gas accretion rates onto Earth-sized planets never exceed disk accretion $\dot{M}_{\mathrm{disk}} = 3\pi\nu\Sigma_{\mathrm{gas}}$.[7] Thus, disk dispersal terminates the gas inflow toward a planet.

In this study, we assume that a disk gas freely flows into a planet until atmospheric contraction due to radiative cooling occurs. Recently, Ormel et al. (2015) found that a rapid recycle of the atmospheric gas suppresses gas accretion onto a planet embedded in an isothermal disk, whereas Kurokawa & Tanigawa (2018) showed that the atmospheric recycling of a

---

[7] The supply of a disk gas to an accreting planet may be further limited in a disk wind-driven disk (Ogihara & Hori 2018).

planet should be less efficient in non-isothermal cases because of the buoyancy barrier. In addition, small grains may be suspended in an accreting H_2-rich gas flow, leading to the delay of atmospheric cooling (Lambrechts & Lega 2017). A dusty H_2-rich gas, which is enriched with small grains, causes less efficient gas capture by a planet. As a result, the final amount of a H_2-rich gas accreted on a planet should be reduced in a dusty (or high-metallicity) disk (see also Ikoma & Hori 2012; Lee et al. 2014). If the collisional growth of small grains in the accreted H_2-rich gas, however, proceeds quickly, larger grains (or aggregates) settle down and sublimate near the bottom of the planetary atmosphere (Movshovitz & Podolak 2008). Eventually, the upper atmosphere of a planet becomes grain-depleted. We consider this case in which the accreting disk gas has grain opacities reduced to 1% of the interstellar medium values (Semenov et al. 2003). Although actual grain opacities in an accreting disk gas and the upper atmosphere of a planet are still uncertain, the choice of lower opacities leads to more massive atmospheres, allowing us to estimate upper limits on the mass of an accreted hydrogen-rich gas.

2.4. Atmospheric Escape from a Planet

Close-in planets undergo atmospheric loss by stellar X-ray and UV (XUV) radiation and injection of high-energy particles via a stellar wind and coronal mass ejection. Atmospheric loss from the TRAPPIST-1 planets was recently studied: water loss by XUV irradiation (Bolmont et al. 2017; Bourrier et al. 2017a) and atmospheric ion escape via a stellar wind, assuming Venus-like atmospheres (Dong et al. 2018). In this paper, we further estimate mass loss of a hydrogen-rich atmosphere from TRAPPIST-1-like planets (like those in the TRAPPIST-1 system) via energy-limited hydrodynamic escape (e.g., Watson et al. 1981).

The hydrodynamic mass loss rate from a planet is given by

$$\dot{M}_{\mathrm{esc}} = \frac{\eta F_{\mathrm{XUV}} \pi R_{\mathrm{XUV}}^3}{G M_{\mathrm{p}} K_{\mathrm{tide}}}, \tag{7}$$

where $\dot{M}_{\mathrm{esc}}$ is the mass loss rate, F_{XUV} is the incident XUV flux, G is the gravitational constant, R_{XUV} is the planetary radius at which the H/He atmosphere becomes optically thick to XUV photons, K_{tide} is the correction factor due to the effects of stellar tidal forces (Erkaev et al. 2007), and η is the heating efficiency by stellar XUV radiation, which is defined as the ratio of kinetic energy of photoelectrons to the absorbed XUV energy. We assume that $R_{\mathrm{XUV}} \sim R_{\mathrm{p}}(t)$ for TRAPPIST-1-like planets (Lopez & Fortney 2014), where $R_{\mathrm{p}}(t)$ is the planetary radius as a function of time t. We define R_{p} as the photosphere, i.e., $R_{\mathrm{p}} = R_{\mathrm{bc}} + R_{\mathrm{atm}}$, where R_{bc} is the radiative–convective boundary and R_{atm} is the photospheric correction given in Lopez & Fortney (2014). As outer boundary conditions for an evaporating planet after disk dissipation, it has an equilibrium temperature at the radiative–convective boundary above which it is assumed to be isothermal. We use the equilibrium temperatures of the TRAPPIST-1 planets given in Gillon et al. (2017). We calculate $R_{\mathrm{bc}}(t)$ by integrating the interior structure of a planet undergoing an atmospheric mass loss at a given t, using Equations (3)–(7). We model the interior structure of a planet with a hydrogen-rich atmosphere using the SCvH equation of state (Saumon et al. 1995). The core is assumed to

be rocky material with a constant density in this study. We compute the thermal evolution of a planet for the age of TRAPPIST-1. The heating efficiency for hydrogen-dominated upper atmospheres never exceeds 20% (Shematovich et al. 2014; Ionov & Shematovich 2015; Ionov et al. 2018). Owen & Jackson (2012) demonstrated that heating efficiencies for Earth-sized planets were low ($\eta \sim 0.1$–0.15). Thus, we adopt a constant $\eta = 0.1$, although η certainly varies with time.

The time evolution of the XUV flux from TRAPPIST-1 remains poorly understood. We adopt a scaling law of X-ray luminosities for M-dwarfs with ages of 5–740 Myr found in Jackson et al. (2012):

$$L_{\mathrm{XUV}}(t) = \begin{cases} L_0, & t \leqslant 100 \text{ Myr} \\ L_0\left(\dfrac{t}{100 \text{ Myr}}\right)^{-1.2}, & t > 100 \text{ Myr}, \end{cases} \tag{8}$$

where L_{XUV} is the XUV luminosity of the star, t is the age, and L_0 is the saturated XUV luminosity. The current XUV flux from TRAPPIST-1 was derived from *XMM-Newton* (Wheatley et al. 2017), $L_{\mathrm{XUV}}/L_{\mathrm{bol}} \sim 6$–$9 \times 10^{-4}$, and *HST*/STIS observations (Bourrier et al. 2017a, 2017b), $L_{\mathrm{XUV}}/L_{\mathrm{bol}} \sim 2$–$4 \times 10^{-4}$, where L_{bol} is the bolometric luminosity of TRAPPIST-1.

The age of TRAPPIST-1 was estimated to be $\sim$3–8 Gyr from the rotational period of $\sim$3.3 days (Luger et al. 2017). Burgasser & Mamajek (2017) concluded that TRAPPIST-1 is a thin/thick disk star with an age of 7.6 ± 2.2 Gyr based on the analyses of Li abundance, metallicity, rotation, and *UVW* velocities (Burgasser & Mamajek 2017). Despite the old age of TRAPPIST-1, frequent strong flare events (Vida et al. 2017) and strong X-ray and EUV (XUV) emissions (Wheatley et al. 2017) from TRAPPIST-1 have been observed. The ratio of Lyα to X-ray emission from TRAPPIST-1 suggests that its chromosphere is moderately active compared to its corona and transition region (Bourrier et al. 2017b). Considering that the age of TRAPPIST-1 is 7.6 ± 2.2 Gyr (Burgasser & Mamajek 2017), we determine the saturated XUV luminosity of TRAPPIST-1: $L_0 \sim 4.7 \times 10^{-5} L_{\odot}$ for $L_{\mathrm{XUV}}/L_{\mathrm{bol}} = 5 \times 10^{-4}$.

3. Results

3.1. Disk Gas Accretion In Situ and during Migration

Figure 1 shows the atmospheric growth of a migrating and a non-migrating planetary core with mass $0.3 M_{\oplus}$ (for TRAPPIST-1 d, 1 h), $0.7 M_{\oplus}$ (for 1 e), and $1 M_{\oplus}$ (for 1 b, 1 c, 1 f, and 1 g) in a steady-state accretion disk. The initial locations of non-migrating planetary cores adopt the orbital configuration of the TRAPPIST-1 planets, whereas a migrating one starts to move inward from 0.1 au or 0.2 au. Atmospheric loss from a planet driven by a stellar XUV irradiation is not included while gas accretion onto it proceeds. We consider that small grains in an accreted hydrogen-rich envelope are highly depleted.

We see a stepwise atmospheric growth of a planetary core. As a migrating core approaches a central star, its atmospheric mass begins to decrease because the Hill radius shrinks and the temperature of the ambient disk gas increases. As a result, an inner planet accretes disk gas less efficiently, as seen in Figure 1. After a migrating core gets stalled at a given location, it gradually accretes the ambient disk gas in situ, leading to an

upturn in the atmospheric mass. As far as the disk lifetime is longer than the Type I migration timescale, which depends on planetary mass and disk properties, the atmospheric growth of a planetary core should proceed in two phases.

We find that disk evolution in the late stage of disk dispersal (even after $t > \tau_{\rm disk}$) controls the final atmospheric mass of a planetary core because its atmosphere continues to drain away. A decreasing gas density at the disk midplane slows down the envelope growth and finally causes atmospheric loss during disk dissipation. While the atmospheric mass loss occurs, the outer envelope of the planet is almost isothermal. Since the internal energy of the planet is still slowly carried away into space, the surface temperature gradually decreases.

Atmospheric erosion of a planet in the late stage of disk dissipation is sensitive to core mass and disk dissipation timescale (Ikoma & Hori 2012), core cooling (Ginzburg et al. 2016, 2018), and radiative transfer in the atmosphere of a planet (Lee et al. 2018). A close-in massive core, which is typically comparable to a critical core mass or larger, can avoid atmospheric loss even in a dissipating disk (see also Figure 2 of Ikoma & Hori 2012) and retain a massive atmosphere. Shorter disk lifetimes prevent a planet from accreting a significant amount of the disk gas. A rapid decrease in the disk gas density also drives more efficient mass loss of the envelope of a planet. The heat released by a core drives the blow-off of thin atmospheres of TRAPPIST-1-like planets in a disk-depleted environment (Ginzburg et al. 2016). In addition, since radiative cooling in the atmosphere of a planet controls the efficiency of gravitational contraction, atmospheric growth/loss should be dependent on both grain opacities and a detailed thermal profile in the atmosphere above the radiative–convective boundary (Lee et al. 2018). A massive core without a core luminosity never undergoes significant atmospheric loss (see Figure 6 of Lee et al. 2018).

When a planet is detached from the ambient disk or becomes isolated, the remaining hydrogen-rich gas should be the gravitationally bound atmosphere. In this study, we do not simulate the detailed structure of gas flow around a planet in the last stage of disk dispersal. Nevertheless, the maximum mass fractions of an accreted hydrogen-rich atmosphere are estimated to be as small as 10^{-2} wt% and 0.1 wt% for the two inner planets (TRAPPIST-1 b and 1 c), 10^{-2} wt% for 1 d, 1 wt%, a few wt% for the three planets 1 e, 1 f, and 1 g in a conventional habitable zone, and 1 wt% for the outermost planet 1 h.

Even a $1\,M_\oplus$ core fails to acquire a massive hydrogen-rich envelope. A massive core accretes more disk gas, whereby it moves toward a central star faster than a smaller one and the Hill radius decreases. It is hard for a hot disk gas in the vicinity of a star to be gravitationally bound by a planetary core. In other words, the amount of hydrogen-rich gas acquired by a planetary core increases with semimajor axis because of the lower thermal energy of a H_2/He gas and the expansion of the Hill sphere.

After orbital migration stops, the atmospheric growth of a planetary core follows in situ accumulation of a disk gas by itself. Since a disk gas accreted onto a planetary core continues to leak out of the Hill radius with decreasing $\Sigma_{\rm gas}$, the amount of a hydrogen-rich atmosphere is controlled by atmospheric loss, accompanied by disk dissipation. The final atmospheric mass of a migrating planet is comparable to that of a non-migrating planetary core with the same mass that formed in situ

after Type I migration stops. As seen in the TRAPPIST-1 system, if a massive core is captured into resonance with an inner planet during planetary migration, the amount of hydrogen-rich atmosphere should be limited by the resonant location.

3.2. A Rapidly Dissipating Disk

Disk wind may accelerate disk dispersal in the late stage of planet formation (Suzuki & Inutsuka 2009). We consider gas accretion onto a migrating planet in a disk wind-driven accretion disk. Figure 2 shows atmospheric growth of a migrating planet with $0.3\,M_\oplus$ (TRAPPIST-1 h), $0.7\,M_\oplus$ (1 e), and $1\,M_\oplus$ (1 f and 1 g) in a disk wind-driven accretion disk. We see a rapid decline in the atmospheric mass of a planet after $t = \tau_{\rm disk}$ in a disk wind-driven disk. The leakage of a H_2-rich gas out of the Hill radius is susceptible to the decrease in the surface density of the ambient disk gas. Since rapid disk dispersal via disk wind after $t = \tau_{\rm disk}$ accelerates the decrease in density of the ambient disk gas, the amount of H_2-rich gas that is gravitationally bound by a planet is suppressed by this dissipation of disk gas.

3.3. Hydrodynamic Escape of an Accreted Hydrogen-rich Gas

The TRAPPIST-1 planets can have a small amount of H_2-rich atmosphere (10^{-2}–a few wt%) as a consequence of accumulation of a disk gas, as shown in Figure 1. Here we consider a TRAPPIST-1-like planet that retains an accreted hydrogen-rich gas after planet formation, and compute the atmospheric mass loss driven by a stellar XUV irradiation. Figure 3 shows the atmospheric mass of only five TRAPPIST-1-like planets (1 c: 0.1 wt% at 0.158 au, 1 e: 1 wt% at 0.0293 au, 1 f: 2 wt% at 0.0385 au, 1 g: 2 wt% at 0.0469 au, and 1 h: 1 wt% at 0.0619 au) as a function of time. Since the two inner planets (1 b and 1 d) have a small fraction of H_2-rich atmosphere ($\sim 10^{-2}$ wt%), such atmospheres are gone in a few Myr. A smaller core closer to the central star completely loses the accreted H_2-rich atmosphere more rapidly. Even TRAPPIST-1-like planets in a potentially habitable zone and beyond cannot retain their primordial atmospheres for 1 Gyr. Although time evolution of TRAPPIST-1's XUV flux remains poorly understood, all the primordial atmospheres of the TRAPPIST-1 planets are lost to space via hydrodynamic escape driven by stellar XUV irradiation unless TRAPPIST-1 is a young ultracool dwarf aged $\lesssim 1$ Gyr.

4. Discussions

No prominent absorption features at near-infrared wavelengths in the transmission spectra of the atmospheres of the TRAPPIST-1 planets rule out cloud-free, hydrogen-rich atmospheres (de Wit et al. 2016, 2018; Zhang et al. 2018; Burdanov et al. 2019), whereas a clear hydrogen-rich atmosphere for TRAPPIST-1 f and 1 g is still in dispute (de Wit et al. 2018; Moran et al. 2018; Wakeford et al. 2019). Our results show that all the TRAPPIST-1 planets used to have a hydrogen-rich atmosphere of $\lesssim 10^{-2}$–1 wt% just after disk dispersal. All the accreted hydrogen-rich atmospheres of the TRAPPIST-1 planets, however, can hydrodynamically escape by a stellar X-ray and UV (XUV) irradiation from their central star in several 100 Myr, which corresponds to the lower limit of the age of TRAPPIST-1 based on Li I absorption and the rotation period (see Burgasser & Mamajek 2017). These imply that the
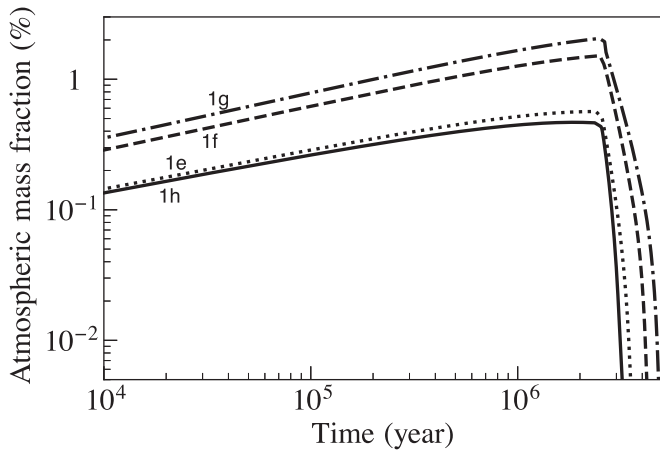
Figure 2. Time evolution of the atmospheric mass fraction of a migrating planetary core with mass of 0.3 $M_\oplus$ (solid: 1 h), 0.7 $M_\oplus$ (dotted: 1 e), 1 $M_\oplus$ (dashed: 1 f and dashed–dotted: 1 g) in a disk wind-driven disk. A stellar XUV-driven atmospheric loss of an accreting planet is not included.
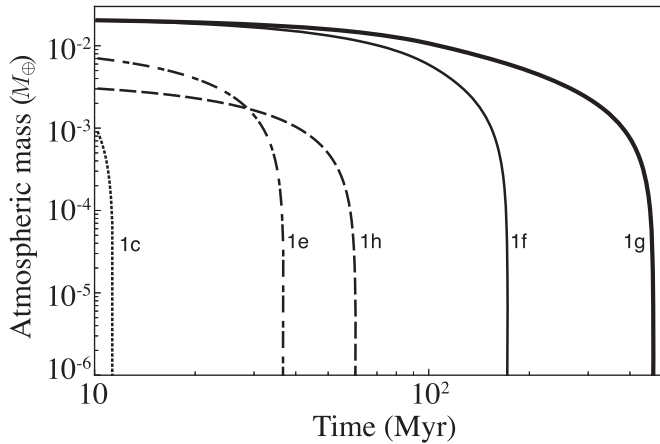

Figure 3. Time evolution of the atmospheric mass of TRAPPIST-1-like planets under stellar XUV radiation. Each planet has initially the maximum amount of hydrogen-rich atmosphere, as shown in Figure 1 : TRAPPIST-1 c (0.1 wt% at 0.158 au: dotted), 1 e (1 wt% at 0.0293 au: dashed–dotted), 1 f (2 wt% at 0.0385 au: thin solid), 1 g (2 wt% at 0.0469 au: thick solid), and 1 h (1 wt% at 0.0619 au: dashed).

TRAPPIST-1 planets, including TRAPPIST-1 g, have neither cloud-free nor cloudy/hazy, hydrogen-rich atmospheres. In other words, if the TRAPPIST-1 planets currently more or less retain atmospheres, these likely originated from secondary processes such as volcanic activities and outgassing.

Recently, interior modeling of the TRAPPIST-1 planets predicts that they may contain water of ≲25 wt% (Quarles et al. 2017; Dorn et al. 2018; Grimm et al. 2018; Suissa & Kipping 2018; Unterborn et al. 2018a, 2018b). Since the inner planets (1 b and 1 c) undergo a runaway greenhouse phase, water can be easily be lost to space. If the initial water content of a TRAPPIST-1 planet is as high as 0.1–1 wt%, they can retain a significant amount of water under a strong XUV radiation field of TRAPPIST-1 (Bolmont et al. 2017; Bourrier et al. 2017a). In addition, the TRAPPIST-1 planets can survive atmospheric ion escape (O^+, O_2^+, and CO_2^+) driven by a stellar wind over a few 100 Myr to ~Gyr (Dong et al. 2018). Thus, a Venus-like atmosphere as well water vapor might be a plausible solution to the atmospheric compositions of the TRAPPIST-1 planets, which is favored by their flat and featureless transmission spectra. If the TRAPPIST-1 planets

possess terrestrial-like atmospheres containing CO_2, CO_2 absorption will be detectable in transmission spectra acquired in less than 10 transits with *James Webb Space Telescope*/ NIRSpec Prism, although the detection of O_2 and O_3 will still be elusive (Lustig-Yaeger et al. 2019).

5. Summary

We have examined the accumulation of a hydrogen-rich disk gas onto a TRAPPIST-1-like planet that formed in situ and a migrating one with mass 0.3 $M_\oplus$, 0.7 $M_\oplus$, and 1 $M_\oplus$. With updated masses and semimajor axes of the TRAPPIST-1 planets, mass fractions of their hydrogen-rich atmospheres are estimated to be as small as 10^{-2} wt% and 0.1 wt% for TRAPPIST-1 b and 1 c, 10^{-2} wt% for 1 d, 1 wt% for 1 e, a few wt% for 1 f and 1 g and 1 wt% for 1 h. All the accreted hydrogen-rich gases can, however, be lost to space by stellar X-ray and UV irradiation several 100 Myr after disk dispersal. Our results suggest that the present-day TRAPPIST-1 planets have no primordial H_2-rich atmospheres. We confirm that a proposed formation scenario for the TRAPPIST-1 planets is compatible with their transit observations. Thus, featureless transmission spectra in the atmosphere of the TRAPPIST-1 planets with *HST*/WFC3 imply that their atmospheres should be dominated by secondary processes such as volcanic activity and outgassing, namely, a high-metallicity gas accompanied by (no) cloud/haze.

ORCID iDs

Yasunori Hori https://orcid.org/0000-0003-4676-0251
Masahiro Ogihara https://orcid.org/0000-0002-8300-7990

References

Alexander, R., Pascucci, I., Andrews, S., Armitage, P., & Cieza, L. 2014, in Protostars and Planets VI, ed. H. Beuther et al. (Tuczon, AZ: Univ. Arizona Press), 475
Andrews, S. M., Rosenfeld, K. A., Kraus, A. L., & Wilner, D. J. 2013, ApJ, 771, 129
Andrews, S. M., Wilner, D. J., Hughes, A. M., Qi, C., & Dullemond, C. P. 2010, ApJ, 723, 1241
Barr, A. C., Dobos, V., & Kiss, L. L. 2018, A&A, 613, A37
Benítez-Llambay, P., Masset, F., Koenigsberger, G., & Szulágyi, J. 2015, Natur, 520, 63
Bitsch, B., Johansen, A., Lambrechts, M., & Morbidelli, A. 2015, A&A, 575, A28
Bolmont, E., Selsis, F., Owen, J. E., et al. 2017, MNRAS, 464, 3728
Bourrier, V., de Wit, J., Bolmont, E., et al. 2017a, AJ, 154, 121
Bourrier, V., Ehrenreich, D., Wheatley, P. J., et al. 2017b, A&A, 599, L3
Burdanov, A. Y., Lederer, S. M., Gillon, M., et al. 2019, MNRAS, 487, 1634
Burgasser, A. J., & Mamajek, E. E. 2017, ApJ, 845, 110
de Wit, J., Wakeford, H. R., Gillon, M., et al. 2016, Natur, 537, 69
de Wit, J., Wakeford, H. R., Lewis, N. K., et al. 2018, NatAs, 2, 214
Delrez, L., Gillon, M., Triaud, A. H. M. J., et al. 2018, MNRAS, 475, 3577
Dong, C., Jin, M., Lingam, M., et al. 2018, PNAS, 115, 260
Dorn, C., Mosegaard, K., Grimm, S. L., & Alibert, Y. 2018, ApJ, 865, 20
Ducrot, E., Sestovic, M., Morris, B. M., et al. 2018, AJ, 156, 218
Erkaev, N. V., Kulikov, Y. N., Lammer, H., et al. 2007, A&A, 472, 329
Fedele, D., van den Ancker, M. E., Henning, T., Jayawardhana, R., & Oliveira, J. M. 2010, A&A, 510, A72
Frank, J., King, A., & Raine, D. 1992, Accretion Power in Astrophysics (Cambridge: Cambridge Univ. Press)
Gillon, M., Jehin, E., Lederer, S. M., et al. 2016, Natur, 533, 221

Gillon, M., Triaud, A. H. M. J., Demory, B.-O., et al. 2017, Natur, 542, 456
Ginzburg, S., Schlichting, H. E., & Sari, R. 2016, ApJ, 825, 29
Ginzburg, S., Schlichting, H. E., & Sari, R. 2018, MNRAS, 476, 759
Grimm, S. L., Demory, B.-O., Gillon, M., et al. 2018, A&A, 613, A68
Guilera, O. M., Cuello, N., Montesinos, M., et al. 2019, MNRAS, 486, 5690
Guillot, T., Chabrier, G., Gautier, D., & Morel, P. 1995, ApJ, 450, 463
Haisch, K. E., Jr., Lada, E. A., & Lada, C. J. 2001, ApJL, 553, L153
Hernández, J., Hartmann, L., Calvet, N., et al. 2008, ApJ, 686, 1195
Ida, S., Yamamura, T., & Okuzumi, S. 2019, A&A, 624, A28
Ikoma, M., & Hori, Y. 2012, ApJ, 753, 66
Ionov, D. E., Pavlyuchenkov, Y. N., & Shematovich, V. I. 2018, MNRAS,
    476, 5639
Ionov, D. E., & Shematovich, V. I. 2015, SoSyR, 49, 339
Jackson, A. P., Davis, T. A., & Wheatley, P. J. 2012, MNRAS, 422, 2024
Jiménez, M. A., & Masset, F. S. 2017, MNRAS, 471, 4917
Kislyakova, K. G., Noack, L., Johnstone, C. P., et al. 2017, NatAs, 1, 878
Kral, Q., Wyatt, M. C., Triaud, A. H. M. J., et al. 2018, MNRAS, 479, 2649
Kratter, K., & Lodato, G. 2016, ARA&A, 54, 271
Kurokawa, H., & Tanigawa, T. 2018, MNRAS, 479, 635
Lambrechts, M., Johansen, A., & Morbidelli, A. 2014, A&A, 572, A35
Lambrechts, M., & Lega, E. 2017, A&A, 606, A146
Lambrechts, M., Morbidelli, A., Jacobson, S. A., et al. 2019, A&A, 627, A83
Lee, E. J., Chiang, E., & Ferguson, J. W. 2018, MNRAS, 476, 2199
Lee, E. J., Chiang, E., & Ormel, C. W. 2014, ApJ, 797, 95
Lin, D. N. C., & Papaloizou, J. C. B. 1993, in Protostars and Planets III, ed.
    E. H. Levy & J. I. Lunine (Tucson, AZ: Univ. Arizona Press), 749
Lopez, E. D., & Fortney, J. J. 2014, ApJ, 792, 1
Luger, R., Sestovic, M., Kruse, E., et al. 2017, NatAs, 1, 0129
Lustig-Yaeger, J., Meadows, V. S., & Lincowski, A. P. 2019, AJ, 158, 27
Mamajek, E. E. 2009, in AIP Conf. Ser. 1158, Exoplanets and Disks: Their
    Formation and Diversity, ed. T. Usuda, M. Tamura, & M. Ishii (Melville,
    NY: AIP), 3
Manara, C. F., Testi, L., Natta, A., & Alcalá, J. M. 2015, A&A, 579, A66
Masset, F. S. 2017, MNRAS, 472, 4204
Matsumoto, Y., Nagasawa, M., & Ida, S. 2012, Icar, 221, 624
Ribas, Á., Merín, B., Bouy, H., & Maud, L. T. 2014, A&A, 561, A54
Mills, S. M., Fabrycky, D. C., Migaszewski, C., et al. 2016, Natur, 533, 509
Moran, S. E., Hörst, S. M., Batalha, N. E., Lewis, N. K., & Wakeford, H. R.
    2018, AJ, 156, 252

Morley, C. V., Fortney, J. J., Marley, M. S., et al. 2015, ApJ, 815, 110
Morris, B. M., Agol, E., Davenport, J. R. A., & Hawley, S. L. 2018a, ApJ,
    857, 39
Morris, B. M., Agol, E., Hebb, L., et al. 2018b, ApJL, 863, L32
Movshovitz, N., & Podolak, M. 2008, Icar, 194, 368
Ogihara, M., & Hori, Y. 2018, ApJ, 867, 127
Ogihara, M., Kokubo, E., Suzuki, T. K., & Morbidelli, A. 2018, A&A,
    615, A63
Ormel, C. W., Liu, B., & Schoonenberg, D. 2017, A&A, 604, A1
Ormel, C. W., Shi, J.-M., & Kuiper, R. 2015, MNRAS, 447, 3512
Owen, J. E., & Jackson, A. P. 2012, MNRAS, 425, 2931
Papaloizou, J. C. B., Szuszkiewicz, E., & Terquem, C. 2018, MNRAS,
    476, 5032
Quarles, B., Quintana, E. V., Lopez, E., Schlieder, J. E., & Barclay, T. 2017,
    ApJL, 842, L5
Saumon, D., Chabrier, G., & van Horn, H. M. 1995, ApJS, 99, 713
Schoonenberg, D., Liu, B., Ormel, C. W., & Dorn, C. 2019, A&A, 627, A149
Semenov, D., Henning, T., Helling, C., Ilgner, M., & Sedlmayr, E. 2003, A&A,
    410, 611
Shakura, N. I., & Sunyaev, R. A. 1973, A&A, 500, 33
Shematovich, V. I., Ionov, D. E., & Lammer, H. 2014, A&A, 571, A94
Suissa, G., & Kipping, D. 2018, RNAAS, 2, 31
Suzuki, T. K., & Inutsuka, S.-i 2009, ApJL, 691, L49
Suzuki, T. K., Ogihara, M., Morbidelli, A., Crida, A., & Guillot, T. 2016,
    A&A, 596, A74
Tamayo, D., Rein, H., Petrovich, C., & Murray, N. 2017, ApJL, 840, L19
Unterborn, C. T., Desch, S. J., Hinkel, N. R., & Lorenzo, A. 2018a, NatAs,
    2, 297
Unterborn, C. T., Hinkel, N. R., & Desch, S. J. 2018b, RNAAS, 3, 116
Van Grootel, V., Fernandes, C. S., Gillon, M., et al. 2018, ApJ, 853, 30
Vida, K., Kővári, Z., Pál, A., Oláh, K., & Kriskovics, L. 2017, ApJ, 841, 124
Wakeford, H. R., Lewis, N. K., Fowler, J., et al. 2019, AJ, 157, 11
Wang, S., Wu, D.-H., Barclay, T., & Laughlin, G. P. 2017, arXiv:1704.04290
Watson, A. J., Donahue, T. M., & Walker, J. C. G. 1981, Icar, 48, 150
Wheatley, P. J., Louden, T., Bourrier, V., Ehrenreich, D., & Gillon, M. 2017,
    MNRAS, 465, L74
Zhang, Z., Zhou, Y., Rackham, B. V., & Apai, D. 2018, AJ, 156, 178